

Influence of post-growth treatment on the optical properties of In:Ce:Cu:LiNbO₃ crystals

Wei Yuan^a, Biao Wang^{a,b,*}, Decai Ma^a, Rui Wang^a

^aHarbin Institute of Technology, Harbin 150001, China

^bSun Yat-Sen University, Guangzhou 510275, China

Received 27 November 2007; accepted 20 April 2008

Abstract

Congruent In (3 mol%):Ce:Cu:LiNbO₃ crystals have been grown by the Czochralski method in air. Some crystal samples were reduced in Li₂CO₃ power, and others were oxidized in Nb₂O₅ power. The structure of crystals was studied by an infrared transmittance spectrum. The resistance ability to optical damage and the photorefractive properties were measured by light-induced scattering experiments and two-beam coupling, respectively. It has been found that the reduction treatment increased the photoconductivity, which resulted in decreased erasure time and diffraction efficiency, but higher light-induced scattering resistance ability. The oxidation treatment caused the inverse affect. Finally, the nonvolatile holographic recording in In:Ce:Cu:LiNbO₃ crystals is realized.

© 2008 Elsevier GmbH. All rights reserved.

Keywords: In:Ce:Cu:LiNbO₃; Post-treatment; Diffraction efficiency

1. Introduction

LiNbO₃ (LN) crystals were widely used in many areas because of their excellent piezoelectric, electro-optic and nonlinear optic properties [1,2]. Because of its excellent photorefractive properties, LN crystals can be applied in many areas, such as piezoelectric, electro-optic, surface acoustic wave, waveguide and nonlinear optical devices [3–6]. However, optical damage and long response time severely limited its applications in practice. The essential way to solve these problems is to optimize the crystal itself by doping with damage-resistance elements (Zn, In, Mg, Sc, etc.) [7–11] and photorefractive sensitivity elements (Fe, Ce, Mn, Cu, etc.) [12–15]. In addition,

moderate post-treatment processes of oxidation and reduction can also change the photorefractive properties of the crystals. To obtain good photorefractive properties by different dopants and post-treatment have attracted much attention in holographic optical data storage.

Liu [16] et al. found that nonvolatile holographic recording can be realized in Ce:Cu:LN crystals. But the recording time was long, doped In ions can improve these properties and moderate post-treatment processes may obtain good photorefractive properties. We obtained a series of high-quality doped In:Ce:Cu:LN crystals grown from the congruent composition, and studied their photorefractive properties after different treatments (oxidation, reduction). On the basis of experimental results, the dependence of the optical damage resistance and photorefractive response time on the defect structure are discussed.

*Corresponding author at: Sun Yat-Sen University, Guangzhou 510275, China. Tel.: +86 2084115692; fax: +86 2084115692.

E-mail address: yw_kjx@163.com (B. Wang).

2. Experimental procedure

2.1. Crystal growth and sample preparation

$\text{In}(3 \text{ mol}\%):\text{Ce}(0.1 \text{ wt}\%):\text{Cu}(0.02 \text{ wt}\%):\text{LiNbO}_3$ single crystals were grown in an automatic diameter control system by the Czochralski method using an intermediate frequency (IF) furnace. The raw materials used to grow the crystals were Li_2CO_3 , Nb_2O_5 , In_2O_3 , CeO_2 and CuO . All raw materials were of 99.99% purity. The Li/Nb ratio of the initial melts to grow the congruent LiNbO_3 is 0.946. The crystals were grown along the c -axis in air from the polycrystalline material in a diameter-controlled equipment at a rate of 2 mm/h and a rotating rate of 15–25 rpm. The growth temperature gradient of the IF furnace was 35–40 °C/cm. After growth, the crystals were cooled down to room temperature at a speed of 50 °C/h. They were then polarized in another furnace, where the temperature gradient was almost zero with a DC electric density of 5 mA/cm² for 30 min. Finally, the crystals were y -cut into slices with the size of $10 \times 2 \times 10 \text{ mm}^3$ ($a \times b \times c$). Some of the samples were buried in Li_2CO_3 power to be reduced at 550 °C for 30 h, and some were buried in Nb_2O_5 power to be oxidized at 1150 °C for 15 h. All the samples were polished by SiC power to optical-grade smoothness.

2.2. Measurements

The IR transmittance spectra of the crystals were recorded with a Fourier spectrophotometer at room temperature. The measurement wave number range was from 3300 to 3600 cm⁻¹.

To measure the diffraction efficiency and the erasure time, the two-wave coupling method was carried out. A scheme of experimental set-up is shown in Fig. 1. The holographic gratings were written by two extraordinarily polarized beams, the wavelength of the laser is 532 nm. After the grating was built, the S beam was blocked and we obtained the

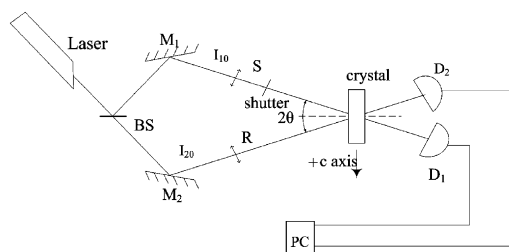


Fig. 1. Experimental set-up of detect diffraction efficiency: BS: beam splitter; M1, M2: mirrors; D1, D2: detector; S: signal beam; R: reference beam; PC: computer.

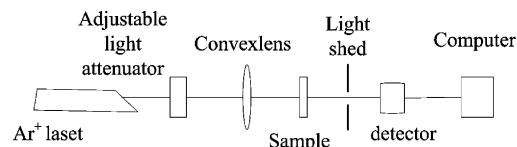


Fig. 2. Experimental set-up for photo scattering resistance ability.

diffraction efficiency:

$$\eta = \frac{I_d}{I_d + I_t}$$

where I_t is the transmitting intensity of the signal beam before the grating was built, and I_d is the diffractive intensity of the signal beam after the grating was built.

Light-induced scattering was used to characterize the resistance ability to the optical damage for crystals. It was performed with a He–Ne laser at the wavelength of 632.8 nm. An attenuator could adjust the laser incident power, and the beam polarizing direction was parallel to the c -axis. The crystals were placed on the focal plane of the convex lens; the central power density of the transmitted beam was record with a detector. Fig. 2 shows the experimental set-up.

3. Results and discussions

3.1. Infrared transmittance spectra

Because of H_2O vapor in the air, H^+ ions were introduced into the crystals during the growth process and formed the O–H band. We can analyze the change of the OH^- absorption peak to conjecture the position of doped ions. The infrared transmittance spectra of crystals are shown in Fig. 3. The OH^- absorption peak of the $\text{Ce}:\text{Cu}:\text{LiNbO}_3$ crystal is located at 3484 cm^{-1} [17]. When the In^{3+} concentration is above its threshold concentration, a part of In^{3+} ions begin to occupy Nb sites and exist in the form of $\text{In}_{\text{Nb}}^{2+}$. Because $\text{In}_{\text{Nb}}^{2+}$ had a higher ability to attract H^+ than that of Li vacancies, OH^- vibration needs more energy, the absorption edges of the crystal shift to short wavelength, which is responsible for the absorption peak at 3508 cm^{-1} . After treatment, the position of the absorption peaks of $\text{In}(3 \text{ mol}\%):\text{Ce}:\text{Cu}:\text{LiNbO}_3$ is just equal to that of as-grown. The treatments seem to have little influence on the position of absorption peaks; this indicates that the post-grown treatments do not influence the defect structure of $\text{In}(3 \text{ mol}\%):\text{Ce}:\text{Cu}:\text{LiNbO}_3$. This indicates that the In concentration in crystals is over the threshold and the post-grown treatments do not influence the defect structure.

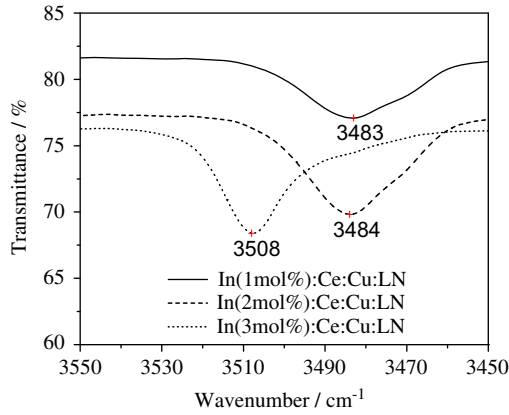


Fig. 3. Infrared transmittance spectra of In:Ce:Cu:LiNbO₃.

3.2. Diffraction efficiency

Using the Kogelnik formula [18], the diffraction efficiency can be

$$\eta_{\max} = \sin^2 \left(\frac{\pi d \Delta n_{\text{sat}}}{\lambda \cos \theta} \right) \quad (1)$$

where η_{\max} is the maximum of diffraction efficiency, d is the sample thickness, λ is the light wavelength, θ is the half angle of incident lights, the saturated photorefractive index change Δn_{sat} can be calculated. The erasure time constant can be obtained by fitting the experimental data with the exponential function, the results are listed in Table 1.

Because the donor concentration decreased by the oxidization process, the photoconductivity of the crystal becomes smaller. According to the expression $\delta \Delta n = (n_e^3) [K j_{\text{ph}} / (\sigma_d + \sigma_{\text{ph}})]$ [19], where n_e is the extraordinary light refractive index, K is the electro-optical coefficient, j_{ph} is the photogalvanic current, σ_d and σ_{ph} are the dark conductivity and photoconductivity. As the photoconductivity of the crystal is changed, the saturated photorefractive index change of the oxidized sample is much higher than that of the as-grown and reduced samples.

3.3. Dependence of photoconductivity on light intensity

It is well known that when laser irradiated the photorefractive crystals, the response time τ_R could be expressed as [20] $\tau_R = \varepsilon \varepsilon_0 / (\sigma_{\text{ph}} + \sigma_d)$, where ε_0 and ε are the dielectric constant in vacuum and the relative dielectric constant. In the range of light intensity studied, σ_d can be neglected in our experiment, $\tau_R = \varepsilon \varepsilon_0 / \sigma_{\text{ph}}$; so the response time was only dependent on the photoconductivity σ_{ph} .

Table 1. Photorefractive properties for In:Ce:Cu:LiNbO₃ crystals under different treatments

State	Δn (10^{-5})	η_{\max} (%)	τ_e (s)
Oxidation	4.5	15	550
As-grown	3.8	10.3	320
Reduction	2.7	8.5	43

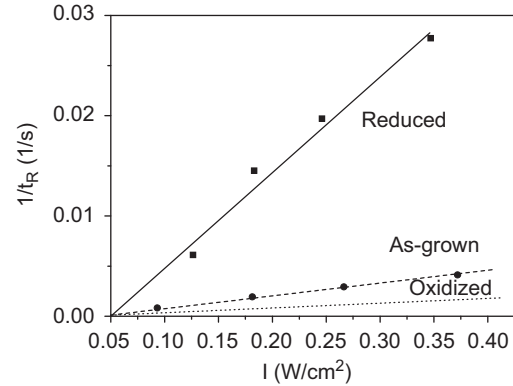


Fig. 4. Dependence of erasure time on different light intensities. (The lines are linear fits to the measured values.)

The diffusion field in the crystals was [21]

$$E_{\text{sc}}(x, t) = E_{\text{sc}}(x) \exp(-\sigma_{\text{ph}} t / \varepsilon \varepsilon_0) \quad (2)$$

The square root of diffraction efficiency was almost directly proportional to the diffusion field. So

$$\frac{\partial}{\partial t} \left(\ln \frac{\eta}{\eta_0} \right) = \frac{2\sigma_{\text{ph}} t}{\varepsilon \varepsilon_0} \quad (3)$$

Thus the photoconductivity could be derived from the straight slope $2\sigma_{\text{ph}} / \varepsilon \varepsilon_0$ of the rectilinear $\ln(\eta/\eta_0)/t$ by the least-squares method. The same as the light intensity dependence of the photoconductivity can be determined by measuring the erasure time at different light intensities. The photoconductivity of the samples was calculated by the erasure curve. The experimental results are shown in Fig. 4.

It is observed that the photoconductivity was proportional to the light intensity. It has been demonstrated that when one energy level to join in the photorefractive process in the LiNbO₃ crystal exists, the photoconductivity is linear with the light intensity. There were two photorefractive centers in the In:Ce:Cu:LiNbO₃ crystals, so it implied that there is only one energy level taking part in the photorefractive process. The photoconductivity of the reduced crystal is the highest, that of the as-grown is bigger and that of the oxidized is smallest. In In:Ce:Cu:LiNbO₃ crystals, Ce^{4+} and Cu^{2+} are the dominant electron acceptors, and they are the most probable electron donors. The donors of the reduced sample are higher than that of the oxidized and the as-grown samples. According to the formula

$\sigma_{ph} = e\mu_e N_e [22]$, where e is the electronic charge, μ_e is electron mobility, N_e is average electron concentration in the conduction band. The reduction treatment increased the photoconductivity and photoconductivity inverse ratio to the erasure time; it also indicated that performing the reduction treatment can shorten the response time.

3.4. Light-induced scattering

The light-induced scatter ability resistance is defined as the ratio R of the light-scattering noise intensity I' and the incident light intensity I . Fig. 5 shows that the results of R depend on the incident light intensity. It can be seen from Fig. 5 that the light-induced scattering resistance ability is increased significantly by doping In in comparison with that of the Ce:Cu:LiNbO₃ crystal. Only when the incident light intensity reached a certain value, the light-induced scatter occurred. The reduction treatment increases the light-scattering resistance ability; on the contrary, the oxidation treatment made it decrease in comparison with that of the as-grown. Because the photorefractive index change is proportional to the ratio of photovoltaic current to the photoconductivity [23], the reduction treatment increased the photoconductivity because of less electron traps of Ce⁴⁺ and Cu²⁺ and larger carrier mobility (Figs. 6 and 7).

4. Nonvolatile two-color holographic storage

The energy level of Cu in LiNbO₃ cannot be excited by He–Ne light. Therefore, the two-color holographic storage can be achieved by the process of UV light sensitizing and red light recording. The crystals were pre-exposed to the UV light (wavelength 365 nm, intensity 30 mW/cm²) for 1 h. Two extraordinary polarization coherent beams (wavelength 632.8 nm,

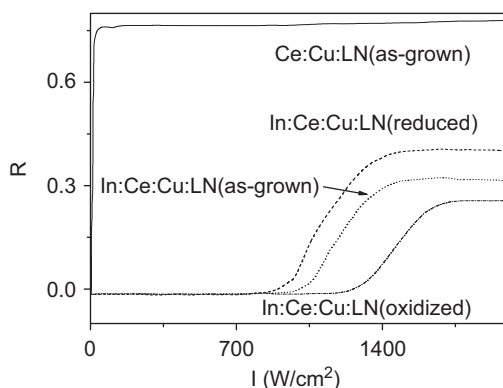


Fig. 5. Incident light intensity dependence of light-scattering noise for different treatments of In:Ce:Cu:LiNbO₃ crystals.

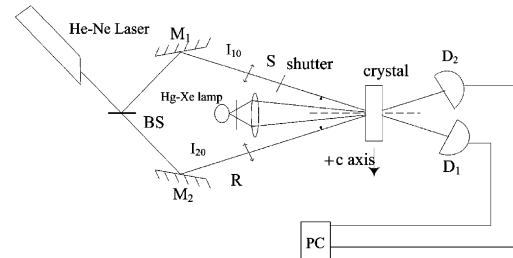


Fig. 6. Sketch of the two-color holographic storage experiment. BS: beam splitter; M1, M2: mirrors; D1, D2: detector; S: signal beam; R: reference beam; PC: computer.

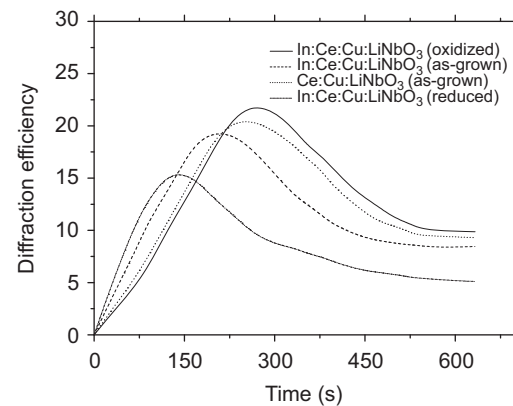


Fig. 7. Dependence of the diffraction efficiency on time.

intensity 15 mW/cm²) originating from a He–Ne laser were incident on the crystals symmetrically, together with UV light. All the crystals are of 3 mm thickness and the c -axis is parallel to the grating vector. The diffraction efficiency was defined as the ratio between diffractive and transmitting intensities, and only red light was used during the readout process. Fig. 5 shows the evolution of diffraction efficiency during recording and readout process.

As shown, the red light only erases the grating recorded in the shallow level, the grating recorded in the deep level will be nonvolatile. The reduction treatment shortens the recording time and decreases the maximum diffraction efficiency, the oxidation treatment made it reverse in comparison with that of the as-grown. The reason for the difference may be that the reduction treatment decreased the electron traps of Ce⁴⁺ and Cu²⁺ and larger carrier mobility.

5. Conclusion

The infrared transmittance spectra indicated that the defect structures were almost not influenced by the post-treatment. But reduction treatments changed the photoconductivity of crystals, which results in shorter respond time and lower diffraction efficiency, and higher

light-induced scattering resistance ability than that of the as-grown. The oxidized treatment increased the diffraction efficiency and respond time, and lower the light-induced scattering resistance ability than that of the as-grown.

Acknowledgments

This work was supported by the National Natural Science Foundation of China (50232030, 10172030), The National Science Foundation of Heilongjiang Province, The Ministry of Science and Technology of China through the High-Tech Program (2001AA31304), and the National Committee of Defence, Science and Technology.

References

- [1] T.Y. Fan, et al., Nd:MgO:LiNbO₃ spectroscopy and laser devices, *J. Opt. Soc. Am. B* 3 (1986) 140–148.
- [2] E. Lallier, J.P. Pocholle, M. Papuchon, M. Mecheli, M.J. Li, Q. He, D.B. Ostrowsky, Nd:MgO:LiNbO₃ waveguide laser and amplifier, *Opt. Lett.* 15 (1990) 682–684.
- [3] Y. Wang, Y.J. Jiang, Crystal orientation dependence of piezoelectric properties in LiNbO₃ and LiTaO₃, *Opt. Mater.* 23 (2003) 403–408.
- [4] K. Chah, M. Aillerie, M.D. Fontana, G. Malovichko, Electro-optic properties in Fe-doped LiNbO₃ crystals as a function of composition, *Opt. Commun.* 176 (2000) 261–265.
- [5] A. Holm, Q. Stürzer, Y. Xu, R. Weigel, Investigation of surface acoustic waves on LiNbO₃, quartz, and LiTaO₃ by laser probing, *Microelectron. Eng.* 31 (1996) 123–127.
- [6] Y.N. Korkishko, V.A. Fedorov, Theoretical analysis of Cherenkov frequency-doubling in a periodically poled LiNbO₃ waveguide, *Opt. Mater.* 5 (1996) 175–185.
- [7] J.J. Liu, W.L. Zhang, G.Y. Zhang, Microscopic mechanism of suppressing photorefractive in LiNbO₃:Mg,Fe crystals, *Solid State Commun.* 98 (1996) 523–526.
- [8] T. Zhang, B. Wang, F.R. Ling, Growth and optical property of Mg, Fe co-doped near-stoichiometric LiNbO₃ crystal, *Mater. Chem. Phys.* 83 (2004) 350–353.
- [9] T.R. Volk, N.V. Razumovski, A.V. Mamaev, N.M. Rubinina, Hologram recording in Zn-doped LiNbO₃ crystals, *J. Opt. Soc. Am. B* 13 (1996) 1457–1460.
- [10] Y.F. Kong, J.K. Wen, H.F. Wang, New doped lithium niobate crystal with high resistance to photorefraction-LiNbO₃:In, *Appl. Phys. Lett.* 66 (1995) 280–282.
- [11] J.K. Yamamoto, T. Yamazaki, K. Yamagishi, Noncritical phase matching and photorefractive damage in Sc₂O₃:LiNbO₃, *Appl. Phys. Lett.* 64 (1994) 3228–3231.
- [12] K. Bush, L. Hollmann, E. Krazig, High-temperature photorefractive effects LiNbO₃:Fe, *J. Appl. Phys.* 73 (1999) 2709–2713.
- [13] F.R. Ling, B. Wang, Effect of UV light on multiplexing holograms in near-stoichiometric LiNbO₃:Ce:Fe, *Opt. Commun.* 241 (2004) 293–298.
- [14] K.S. Lim, S.J. Taka, S.K. Lee, Grating formation and decay in photochromic Mn, Ce:LiNbO₃, *J. Lumin.* 94–95 (2001) 73–78.
- [15] Y.W. Liu, L.R. Liu, Intensity dependence of two-center non-volatile holographic recording in LiNbO₃:Ce:Cu crystals, *Opt. Commun.* 190 (2001) 339–343.
- [16] Y.W. Liu, L.R. Liu, Non-volatile photorefractive holograms in LiNbO₃:Cu:Ce crystals, *Opt. Lett.* 25 (2000) 908–910.
- [17] D.C. Ma, B. Wang, Influence of post-treatment on optical properties of Sc-Ce-Cu-LN crystals, *Mod. Phys. Lett. B* 21 (2007) 207–214.
- [18] H. Kogelnik, Coupled wave theory for thick holograms gratings, *Bell Syst. Tech. J.* 5 (1969) 2909–2947.
- [19] T. Volk, N. Rubinina, M. Wöhlecke, Optical-damage-resistant impurities in lithium–niobate, *J. Opt. Soc. Am. B* 11 (1994) 1681–1687.
- [20] X.J. Chen, D.S. Zhu, B. Li, T. Ling, Z.K. Wu, Fast photorefractive response in strongly reduced near-stoichiometric LiNbO₃ crystals, *Opt. Lett.* 26 (2001) 998–1000.
- [21] M.P. Bienvu, D. Woodbury, T.A. Robson, Hologram decay in LiNbO₃:Fe with a time varying conductivity, *J. Appl. Phys.* 51 (1980) 4245–4247.
- [22] A. Adibi, K. Bush, D. Psaltis, The role of carrier mobility in holographic recording in LiNbO₃, *Appl. Phys. B: Lasers Opt.* 72 (2001) 653–659.
- [23] Y. Zhang, Y.H. Xu, M.H. Li, Y.Q. Zhao, Growth and properties of Zn doped lithium niobate crystal, *J. Cryst. Growth* 233 (2001) 537–540.